Aerosol Science and Engineering (2022) 6:186–196
https://doi.org/10.1007/s41810-022-00134-9

ORIGINAL PAPER

Impact Assessment of Aerosol Optical Depth on Rainfall in Indian Rural Areas

Sneha Gautam[1] · **Janette Elizabeth**[1] · **Alok Sagar Gautam**[2] · **Karan Singh**[2] · **Pullanikkat Abhilash**[1]

Received: 3 February 2022 / Revised: 4 March 2022 / Accepted: 7 March 2022 / Published online: 29 March 2022

Abstract

Aerosol significantly influences the life cycle of clouds and their formation. Many studies reported worldwide on anthropogenic aerosols and their impact on clouds and their optical properties. Atmospheric remote sensing provides the best way to estimate indirectly air quality surveillance and management in megacities of developing countries like India where many cities have elevated concentration profiles of air pollutants with inadequate coverage of spatial and temporal monitoring. The results of the study highlighted the impact on rainfall patterns due to aerosol optical depth (AOD) and fine particulate matter (PM2.5) for a total of 7 years (2015–2021) over five different Indian rural sites by using MODerate Resolution Imaging Spectroradiometer (MODIS). The AOD (550 nm) and PM2.5 were retrieved from the MODIS sensor Terra satellites and the MEERA 2 model, respectively. Also, we have analyzed in this study the relationship of AOD (550 nm) with PM2.5 and meteorological variables (temperature relative humidity and precipitation) over Indian rural sites during 2015–2021. The maximum concentration of AOD (550 nm) has been measured for Gandhi college (2.94 ± 0.44) and minimum for ARM college (0.01 ± 0.28), while the maximum concentration of PM2.5 has been measured for ARM College 296.37 (μg m^{-3}) and minimum for Karunya University 0.02 (μg m^{-3}). Also, the relation between AOD (550 nm) with total precipitation is measured positively for all locations except Gandhi college whereby PM2.5 associated with total precipitation is measured negatively for all locations except ARM college. Finally, the relationship between PM2.5 and AOD (550 nm) is measured positively in all selected locations except Singhad Institute. The maximum rainfall has been observed for monsoon months (June–August) and post-monsoon months (October) for all locations during the study period. The maximum total precipitation has been measured for Singhad 11,674.7 (mm) and the minimum for Karunya University 4563.41 (mm). However, the results of the study indicated that there was no direct trend observed in AOD in five different selected rural Indian sites.

Keywords $PM_{2.5}$ · Aerosol optical depth · MODIS · Rainfall · Temperature · Relative humidity · Rural sites

Abbreviations

AOD	Aerosol optical depth
MODIS	MODerate Resolution Imaging Spectroradiometer
PM	Particulate matter
AU	Amity University
ARM	ARM College of Engineering and Technology
GEC	Gandhi Engineering College
KU	Karunya University
SI	Singhad Institutes
TRMM	Tropical Rainfall Measuring Mission
RMI	TRMM microwave imager
PR	Precipitation radar
VIRS	Visible and infrared scanner

✉ Sneha Gautam
gautamsneha@gmail.com

✉ Alok Sagar Gautam
phyalok@gmail.com

1 Department of Civil Engineering, Karunya Institute of Technology and Sciences, Coimbatore, Tamil Nadu 641114, India

2 Department of Physics, H.N.B. Garhwal University, Garhwal, Srinagar, Uttarakhand 246174, India

1 Introduction

The amount of water from rainfall is one of the most crucial water cycle and global water components with a significant impact on climate conditions (Copernicus Climate Change Service (C3S) 2017; Kalpana et al. 2020; Gautam et al. 2021a, b, c). Many studies highlighted the possible impact of aerosol on cloud formation and related cycles

(Ramanathan et al. 2005; Ramanathan et al. 2001a, b; Kalpana et al. 2020; Gautam et al. 2021a). Many researchers showed fluctuations in optical properties due to the impact of aerosol generated by anthropogenic activities (Chelani and Gautam 2021; Ackerman et al. 2000; Ramanathan et al. 2001a, b; Kaufman et al. 2005). Aerosol comes from anthropogenic and various natural activities; therefore, it characterizes different chemical constituents (Bisht et al. 2022; Gollakota et al. 2021; Humbal et al. 2018, 2019; Chauhan and Singh 2020, 2021; Ranjan et al. 2007). Hence, it determines the variation of the refractive index of a particular aerosol. Loading of atmospheric pollutants due to modernization and industrialization in the urban and rural atmosphere reported significantly to lead to aerosol and monsoon-related problems, especially in Asian countries such as India, China, Pakistan, Bangladesh, etc. (Chelani and Gautam 2022; Gautam et al. 2021b; Gautam and Chelani 2021; Gautam and Brema 2020). However, the sustainable development of Asian countries and supplies of freshwater probably depends on the heavy monsoon season. Lau et al. (2008) discussed the reported significant loss of human life and properties due to flash floods or prolonged drought through the region's uneven distribution of monsoon rain. Several studies estimated that approximately significant seasonal mean (10%) solar radiation could be reduced by atmospheric aerosol, highlighting global cooling effects at the world (Chung et al. 2005; Ramanathan et al. 2001a, b). In recent years, many researchers (Meehl et al. 2008; Menon et al. 2002) have observed the findings of variation in rainfall patterns in the Asian region due to aerosol radiative forces. Its fundamental research and getting attention (scientific/publically) to understand the behavior of aerosol and its possible impact on water resources and agriculture. The reported literature indicated the total incremental concentration of air pollutants and expected the same over urban and rural Indian regions in the coming future (Ramasubramanian et al. 1988; Gautam et al. 2021a, b, c). Presented study is the new endeavor to rural sites of the Indian region to understand the behavior of aerosol on rainfall patterns in the last 7 years (2015–2021) using satellite observations.

2 Methods

2.1 Site Descriptions

In the presented study, a total of five Indian rural sites (i.e., Amity University, ARM College of Engineering and Technology, Gandhi Engineering Collage, Karunya University,

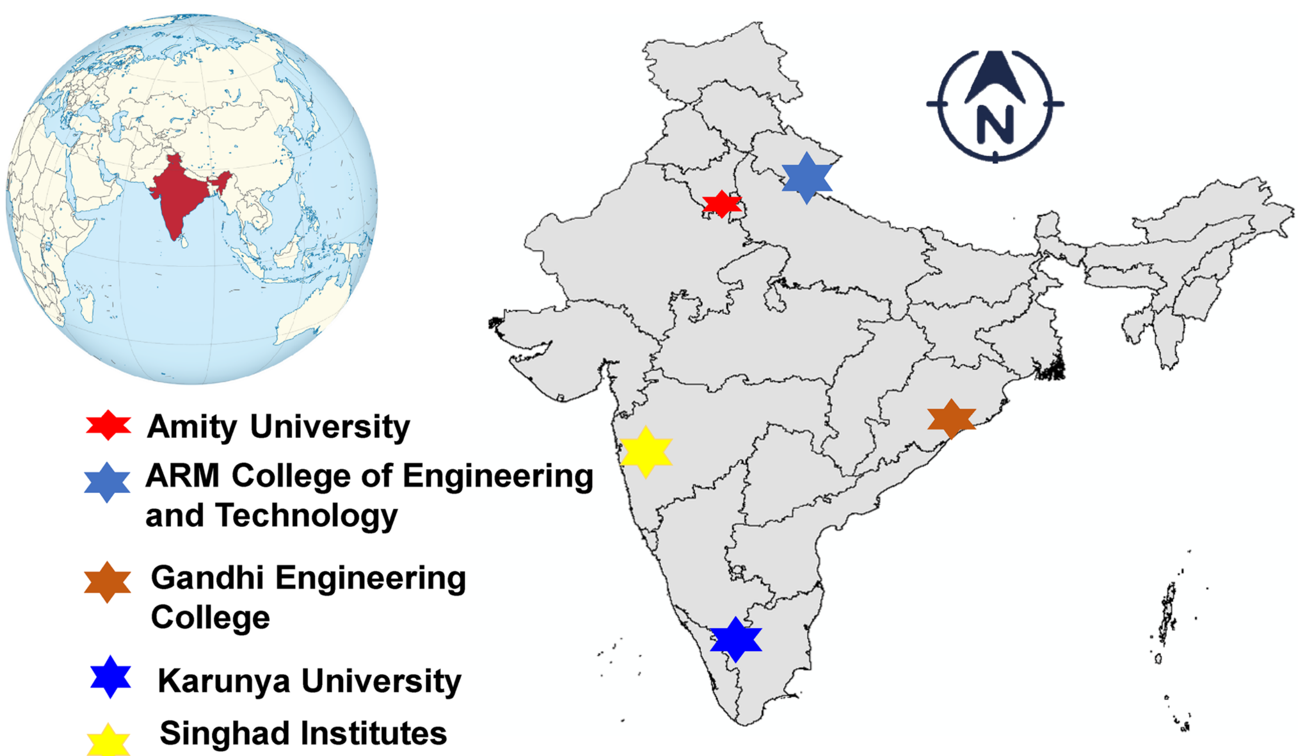

Fig. 1 Study area with selected sampling sites

and Singhad Institutes) were selected according to data availability (Fig. 1).

2.1.1 Amity University (AU)

AU (76.916 E, 28.317 N) is India's largest education group, with over 50,000 students studying across 700 acres of high-tech campus. It is situated in the Pachgaon cluster of villages, Gurgaon, a place in Haryana. The university campus encompasses 110 acres (0.45 km^2), including a 20-acre (81,000 m^2) sports complex. The state's climate is subtropical, semi-arid to sub-humid, continental, and monsoon. Haryana is extremely hot in the summer and extremely cold in the winter. The temperature drops to its lowest point in January and rises to 50 °C in May and June. Rainfall varies, with the Shivalik Hills receiving the most and the Aravali Hills receiving the least.

2.1.2 ARM College of Engineering and Technology (ARM)

ARM (79.458 E, 29.359 N), is located at an elevation (6358 feet) above sea level surrounded by mountains in Nainital (district), Uttarakhand, India. It is situated in the Kumaon foothills of the Himalayan range, 285 km (177 miles) from the state capital of Dehradun. The place has a subtropical highland climate. During the winter, the South Asian monsoon system is quite dry, and during the summer, it is extremely wet. The highest and lowest total precipitation is 725 mm in July (28.5 in) and 7.9 mm (0.31 in) in November, respectively.

2.1.3 Gandhi Engineering College (GEC)

GEC (84.128 E, 25.871 N) is situated in Bhuvneshwar, Odisha. The Institute's campus encompasses a 25-acre plot of land. The place has a tropical savannah climate. The highest and lowest temperature is 46.7 °C (116.1 °F) and 8.2 °C (47 °F), respectively.

2.1.4 Karunya University (KU)

KU (76.744 E, 10.935 N), located in Karunya Nagar with 29.3 km from Coimbatore city, is a nationally ranked, fully residential, private Christian university. It covers 700 acres of land. The place experiences a semi-arid climate. The northeast monsoon causes a wet season in the city from September to November. The highest and lowest average temperature between 35.9 °C (96.6 °F) and 29.2 °C (84.6 °F) and 24.5 °C (76.1 °F) and 19.8 °C (67.6 °F), respectively.

2.1.5 Singhad Institutes (SI)

SI (73.750 E, 18.367 N) is located in Pune, Maharashtra. The campus encompasses 150 acres of lush green land. The climate is tropical wet and dry, bordering on hot semi-arid. The average temperatures ranging between 20 and 28 °C (68-°F and 82-°F).

2.2 Satellite Data

2.2.1 MODerate Resolution Imaging Spectroradiometer (MODIS)

The current study's data on varying aerosol optical depth (AOD) over the selected five rural sites were derived from primarily the Terra satellite. *MODIS* equipment measures cloud droplet distribution and size in ice clouds and liquid water. It gives information about aerosol and its properties, which are microscopic (solid or liquid particles) that exist in the ambient atmosphere.

2.2.2 Tropical Rainfall Measuring Mission (TRMM)

TRMM is a joint program of the US–Japan that uses Precipitation Radar (PR), TRMM Microwave Imager (TMI), and Visible and Infrared Scanner (VIRS) equipment to estimate rainfall (tropical and subtropical). PR analyzed the precipitation column, revealing new tropical storm structure and intensification data.

2.2.3 ERA5 Datasets

We have downloaded the meteorological data, 2-m temperature, relative humidity, and total precipitation in this study. ERA5 provides (1979 to present) hourly estimates of a large number of atmospheric, land, and Oceanic climate variables. The data cover the Earth on a 30 km grid and resolve the atmosphere with 137 levels ranging from the surface to 80 km in altitude. The data are archived in the Meteorological Archival and Retrieval System (MARS) data archive of the European Centre for Medium-Range Weather Forecasts (ECMWF), and a relevant subset of the data has been copied to the C3S Climate Data Store (CDS) discs, interpolated to a regular latitude/longitude grid. On the CDS disks, where single-level and pressure-level data are available, analysis are provided rather than forecasts, unless the parameter is only available from the forecasts.

3 Results

3.1 $PM_{2.5}$

Both natural and human activities cause air pollution in rural areas (Dey et al. 2004). Natural sources of air pollution occur when pollutants are generated from various natural sources (i.e., animals, plants, land resources, forest fires, coal fires, dust storms, volcanic eruptions, and sand storms) and are dispersed in the atmosphere naturally (Arora and Reddy 2013, 2014, 2015; Li et al. 2010). Solid fuel combustion (cooking and heating) as well as agriculture activities, mining (opencast and underground) activities, industrial activities (cement production and coal processing), all contribute significant air pollutants into the ambient atmosphere (Xia et al. 2005). For rural air quality, meteorological factors play an essential role. Factors such as topography, air movement, and climate determine the amount of pollution in the atmosphere at a given time (Gautam et al. 2021a, b, c). Winds play an important role in the deterioration of air pollutants through the dispersal and dilution process. When mountains dominate the topography, winds weaken and calm, and pollutants congregate in the breathing zone, endangering human health. The temperature gradient influences the vertical diffusion of pollutants. When the lower layers of air become rapidly noticeable (temperature inversion), the bit vertical movement of the air and pollutants and water vapors tend to remain trapped at the levels, resulting in 'smog.

In the study, the concentration profile of $PM_{2.5}$ of selected five rural sites of India is presented in Table 1. The $PM_{2.5}$ range (average concentration range ± standard deviation range) of five selected rural sites is AU, ARM, GEC, KU, and SI is (36–24 ± 27–16 μg m^{-3}), (24–13 ± 28–12 μg m^{-3}), (25–15 ± 20–12 μg m^{-3}), (07–04 ± 07–04 μg^{-3}), and (13–08 ± 12–06 μg^{-3}), respectively. One distinct feature was reported in all selected locations in 2018, where the concentration was higher than all remaining years (Table 1). It is observed that from 2015 to 2018, the concentration level was increasing, but it decreased from 2019 to 2020. The reason for the changes may fall under the unwanted pandemic worldwide. However, AU and KU have reported higher concentration (36 ± 27 μg m^{-3}) and lower concentration (04 ± 04 μg m^{-3}) sites during the study periods (Table 1).

3.2 AOD

So far, rural air quality has not been taken as a priority with the common misconception that there is no air pollution in rural areas. On the contrary, the number of developing countries' conditions is worsening due to bad air quality. The indiscriminate use of insecticide/pesticide sprays, as well as the open burning of solid materials (i.e., wheat and paddy

Table 1 Annual statistics of $PM_{2.5}$ from 2015 to 2021 of selected five Indian rural sites

Year	AU		ARM		GEC		KU		SI	
	Mean (μg m^{-3})	SD (μg m^{-3})	Mean (μg m^{-3})	SD (μg m^{-3})	Mean (μg m^{-3})	SD (μg m^{-3})	Mean (μg m^{-3})	SD (μg m^{-3})	Mean (μg m^{-3})	SD (μg m^{-3})
2015	24.37	15.28119	17.82	15.88574	18.52	14.27188	4.95	6.660306	10.36	11.70239
2016	25.78	18.75597	17.65	14.62405	19.68	17.88133	5.22	3.89339	9.14	6.860443
2017	28.97	22.33946	19.87	17.9615	19.15	16.55983	5.75	4.971612	9.71	7.11473
2018	35.91	27.14269	23.27	27.81586	24.26	19.52542	6.60	5.438889	12.57	9.034184
2019	26.62	21.20447	16.86	19.60164	18.84	17.08163	6.36	6.446816	10.03	7.987486
2020	23.18	18.10036	13.48	11.26663	14.66	11.44801	3.95	3.225851	8.00	5.90248
2021	31.44	29.44701	19.26	16.91705	22.74	21.42219	5.10	4.759078	11.39	9.565554

straw), are significant sources of outdoor air pollution. This causes various health issues, primarily affecting the respiratory and cardiovascular systems. Indoor air pollution kills more people than outdoor air pollution. That AU in the year 2018 had faced the maximum amount of AOD (550 nm) and the lowest in the year 2020 (Table 1). Compared to the others, ARM shows a relatively lower value in AOD (550 nm), with its lowest in 2020 with 0.154 and its maximum of 0.236 in 2016. This demonstrates that the global economic and transportation activity has been reduced to unprecedented levels as a result of the coronavirus disease lockdown in 2019 (COVID-19) (see Table 2).

Nevertheless, in GEC, the AOD value was lowest in 2017 with a value of 0.46 and a highest of 0.67 in the year 2016. When ARM and KU are compared, it is clear that the factors that contribute to continuous aerosol loading in the atmosphere are relatively low. Since in all the years, KU has shown a significant dip in the contribution of aerosol loading to the environment. SI had a maximum of 0.2686 in 2018 and a lowest of 0.193 in 2016. Gurgaon has a rainfall pattern that extends to 87 days; this suggests that the increase in AODs may be due to the hygroscopic growth of water-soluble aerosols and the transport of larger-sized aerosols.

Figure 2a demonstrates the daily variation of AOD (550 nm) over India's five most specific colleges and Universities like AU, ARM, GEC, KU, and SI from 1 January 2015 to 30 November 2021. Figure 2a shows the almost similar trend of AOD (550 nm) for all cities every year. The total annual mean of daily AOD (550 nm) concentrations for all five study locations has been measured 0.66 ± 0.37, 0.29 ± 0.28, 0.75 ± 0.44, 0.38 ± 0.21, and 0.39 ± 0.20, respectively, during the course of the research. We have observed from the figure that the daily variation of AOD (550 nm) got highest two times one is winter months Dec–Feb and another is summer months May–June for every year and all locations during the study period. The maximum concentration of AOD has been measured for GEC (0.75 ± 0.44) and the minimum for ARM (0.29 ± 0.28).

Similarly, Fig. 2b demonstrates the daily variation of $PM_{2.5}$ over India's five rural sites from 1 January 2015 to 30 November 2021. Figure 2b shows the almost similar trend of $PM_{2.5}$ for all cities every year. The total annual mean of daily $PM_{2.5}$ concentrations for all five study locations has been measured 28 ± 22.50 (μg m^{-3}), 18.30 ± 18.56 (μg m^{-3}), 19.66 ± 17.32 (μg m^{-3}), 5.42 ± 5.25 (μg m^{-3}), and 10.15 ± 8.59 (μg m^{-3}), respectively, during the study period. The daily variation of $PM_{2.5}$ concentration was observed maximum in 2017–2019 and minimum in 2015, 2016, 2020, and 2021 for all locations. The $PM_{2.5}$ has been distributed differently every year. The variation of $PM_{2.5}$ concentration was observed as maximum for pre-monsoon months from March to May for every year. The maximum concentration of $PM_{2.5}$ has been measured for AU 28 ± 22.50 (μg m^{-3}) and minimum for KU 5.42 ± 5.25 (μg m^{-3}).

Figure 2c demonstrates the daily variation of temperature over study sites from 1 January 2015 to 30 November 2021. The total annual mean of daily variation of temperature for study locations has been measured 25.39 ± 7.22 (°C), 20.35 ± 5.77 (°C), 25.87 ± 6.12 (°C), 25.56 ± 1.75 (°C), and 24.06 ± 2.52 (°C), respectively, during the study period. The daily variation of temperature has a similar trend every year during the study period and got maximum for May–June, while the minimum for December–Jan for all selected observation sites during the study period. The maximum temperature has been measured for GEC 25.87 ± 6.12 (°C) and minimum for ARM 20.35 ± 5.77 (°C).

Figure 2d demonstrates the daily variation of Relative Humidity over India's five rural sites from 1 January 2015 to 30 November 2021. The total annual mean of daily variation of temperature has been measured 50.31 ± 24.84 (%), 64.08 ± 19.62 (%), 59.00 ± 24.88 (%), 74.43 ± 15.39 (%), and 62.75 ± 26.22 (%), respectively, during the study period. The daily variation of relative humidity has a similar trend to the temperature variation, like maximum in May–July and minimum in Dec–Feb for all locations during the study period. The maximum relative humidity has been measured for KU 74.43 ± 15.39 (%) and the minimum for AU 50.31 ± 24.84 (%).

Table 2 Annual statistics of AOD (550 nm) 2015–2021 of selected five Indian rural sites

Year	AU		ARM		GEC		KU		SI	
	Mean	SD	Mean	SD	Mean	SD	Mean	SD	Mean	SD
2015	0.6682	0.403181	0.279287	0.261187	0.774192	0.508919	0.340885	0.188218	0.379437	0.19082
2016	0.692283	0.400672	0.339634	0.362693	0.826754	0.47449	0.447082	0.246194	0.335299	0.177455
2017	0.609018	0.33335	0.259413	0.218737	0.678702	0.354666	0.391987	0.217082	0.388392	0.187867
2018	0.66124	0.345489	0.284437	0.276025	0.75019	0.367977	0.414595	0.239838	0.408846	0.196574
2019	0.664338	0.383327	0.26931	0.268052	0.74689	0.42155	0.368259	0.182257	0.366616	0.183467
2020	0.627309	0.352774	0.231436	0.243872	0.707119	0.403299	0.332967	0.191438	0.386981	0.219812
2021	0.666135	0.39075	0.350113	0.307657	0.8052	0.494592	0.374396	0.20545	0.474249	0.213677

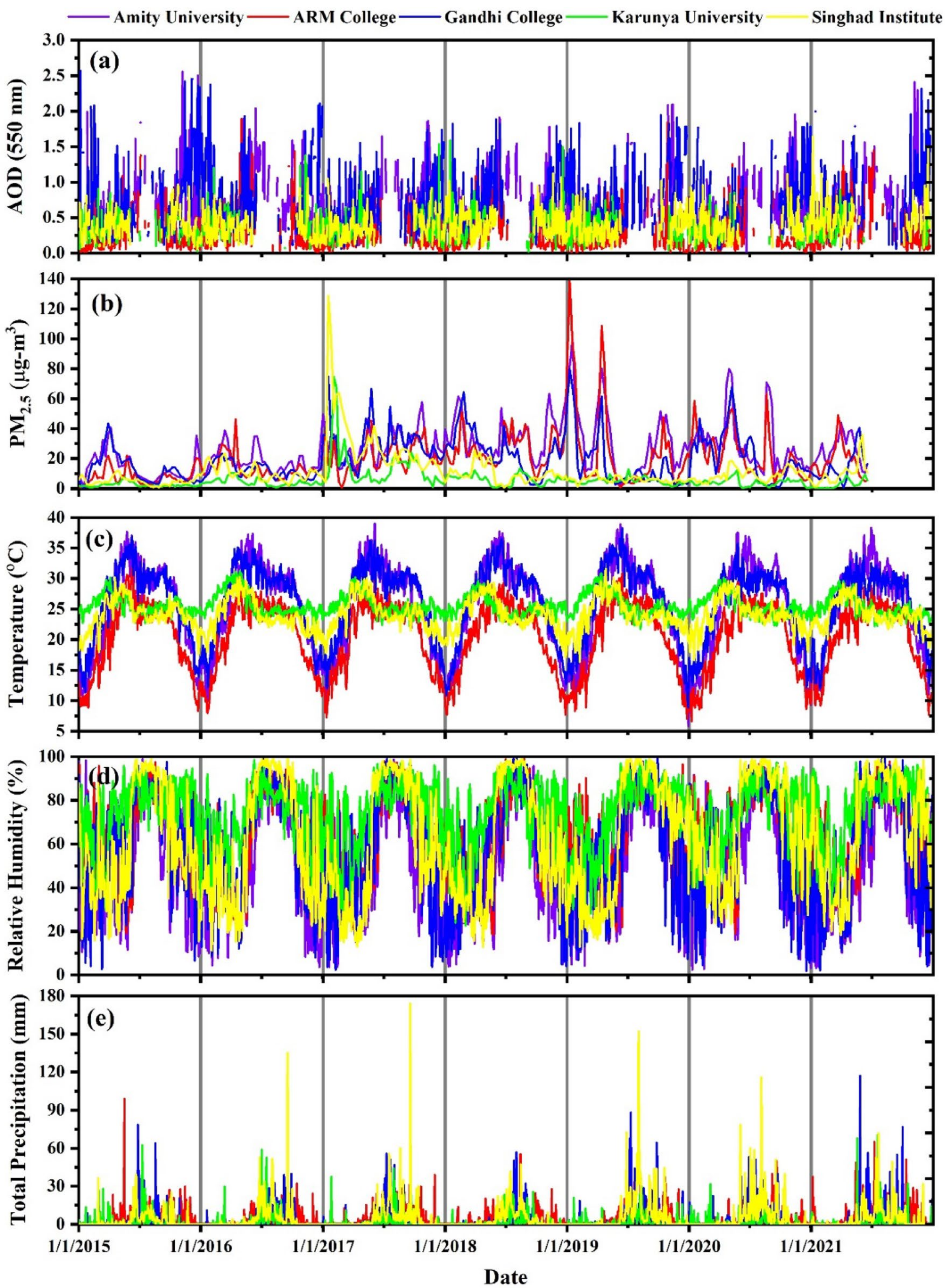

Fig. 2 Temporal variation of AOD (550 nm), PM2.5, temperature, relative humidity, and total precipitation for 2015–2021 over five rural Indian sites

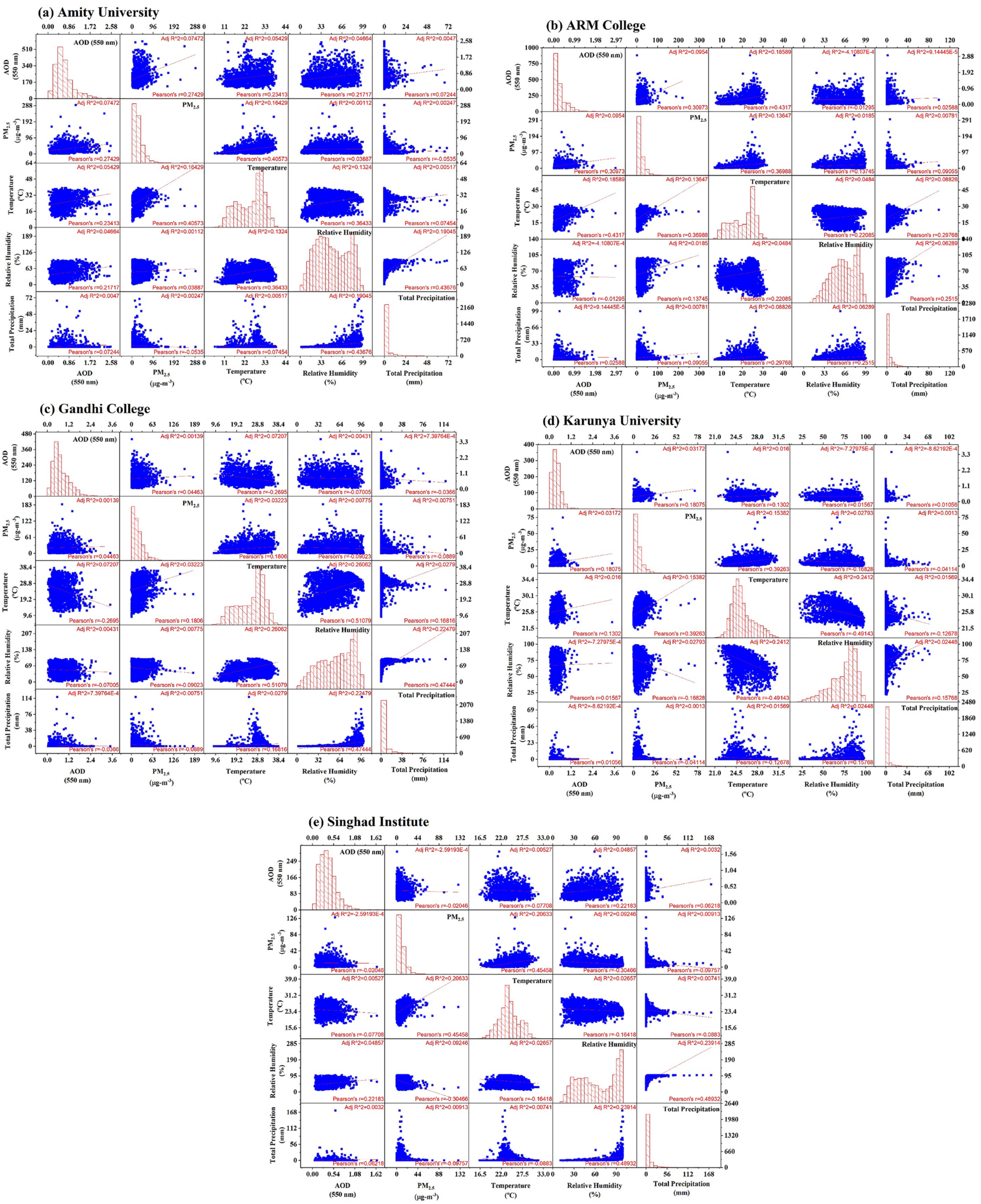

Fig. 3 Correlations among AOD (550 nm), PM2.5, temperature, relative humidity, and total precipitation for all five locations during 2015–2021

Figure 2e demonstrates the daily variation of total precipitation from 1 January 2015 to 30 November 2021 on selected five rural sites. The annual total precipitation has been measured 4563.413 (mm), 10,385.68 (mm), 8747.48 (mm), 4563.413 (mm), and 11,674.7 (mm), respectively. The maximum rainfall has been observed for monsoon months (June–August) and post-monsoon months (October) for all locations during the study period. The maximum total precipitation has been measured for SI 11,674.7 (mm) and the minimum for KU 4563.41 (mm).

Figure 3a demonstrates the relationship among AOD (550 nm), $PM_{2.5}$, temperature, relative humidity, and total precipitation for five rural sites during the study period. The correlations of AOD (550 nm) with $PM_{2.5}$, temperature, relative humidity, and total precipitation have a positive correlation ($r=0.27$), positive correlation ($r=0.23$), positive correlation ($r=0.21$), and positive correlation ($r=0.07$), respectively, for the location of AU and although $PM_{2.5}$ with temperature, relative humidity, and total precipitation have a positive correlation ($r=0.40$), positive correlation ($r=0.03$), and negative correlation ($r=-0.05$) respectively.

Similarly, Fig. 3b demonstrates the relationship among AOD (550 nm), $PM_{2.5}$, and meteorological parameters (i.e., total precipitation, temperature, and relative humidity) for the location of ARM. The correlations of AOD (550 nm) with $PM_{2.5}$, temperature, relative humidity, and total precipitation have a moderate positive correlation ($r=0.30$), moderate positive correlation ($r=0.43$), negative correlation ($r=-0.01$), and positive correlation ($r=0.02$), respectively for the location of ARM college and although $PM_{2.5}$ with temperature, relative humidity, and total precipitation have a moderate positive correlation ($r=0.36$), positive correlation ($r=0.13$), and positive correlation ($r=0.09$), respectively.

Figure 3c demonstrates the relationship among AOD (550 nm), $PM_{2.5}$, temperature, relative humidity, and total precipitation for the location of GEC during the study period. The correlations of AOD (550 nm) with $PM_{2.5}$, temperature, relative humidity, and total precipitation have a positive correlation ($r=0.04$), negative correlation ($r=-0.26$), negative correlation ($r=-0.07$), and negative correlation ($r=-0.03$), respectively, for the location of GEC and although $PM_{2.5}$ with temperature, relative humidity, and total precipitation have a positive correlation ($r=0.18$), negative correlation ($r=-0.09$), and negative correlation ($r=-0.08$), respectively. Figure 3d demonstrates the relationship among AOD (550 nm), $PM_{2.5}$, temperature, relative humidity, and total precipitation for the location of KU during the study period. The correlations of AOD (550 nm) with $PM_{2.5}$, temperature, relative humidity, and total precipitation have a positive correlation ($r=0.18$), positive correlation ($r=0.13$), positive correlation ($r=0.01$), and positive correlation ($r=0.01$), respectively, for the location of KU and although $PM_{2.5}$ with temperature, relative humidity, and total precipitation have a moderate positive correlation ($r=0.39$), negative correlation ($r=-0.16$), and negative correlation ($r=-0.04$), respectively.

Finally, Fig. 3e demonstrates the relationship among AOD (550 nm), $PM_{2.5}$, temperature, relative humidity, and total precipitation for the location of SI during the study period. The correlations of AOD (550 nm) with $PM_{2.5}$, temperature, relative humidity, and total precipitation have a negative correlation ($r=-0.02$), negative correlation ($r=-0.07$), positive correlation ($r=0.22$), and positive correlation ($r=0.06$), respectively, for the location of SI, although $PM_{2.5}$ with temperature, relative humidity, and total precipitation have a moderate positive correlation ($r=0.45$), negative correlation ($r=-0.30$), and negative correlation ($r=-0.09$), respectively.

4 Discussion

The total precipitation has been supporting the increase of AOD (550 nm) values and also with increasing temperature and humidity. It is observed in the monsoon season for all location but for the ARM and SI which are situated in rural area of Nainital and Pune, respectively, had been shown extremely rainfall due to several facts as: (i) high-pressure air masses satisfy a long thermal inversion resulting in high pollutants concentration on the surface (Amarillo et al. 2021; Alfaro et al. 2008); (ii) when the ground surface becomes saturated as a result of recent changes in land cover and land use, some of the air aerosols may be lost along with the precipitation (Tiwari and Singh 2013); (iii) day length and solar heating would be at their highest during the summer months, resulting in significant convective movements and turbulent mixing, and as a result, atmospheric aerosols would be migrating from the lowest level of the land surface to the upper level (He et al. 2014); (iv) this may be attributed to variance in anthropogenic aerosol concentrations from vehicles, factories, and towns (Ramanathan et al. 2001a, b; Kumar 2015); (v) furthermore, In the north of the Indian subcontinent, the Himalayan orography acts as a natural barrier to aerosol dispersion, and low winter temperatures cause aerosol particles to be trapped and accumulated (Xie et al. 2011; Kumar 2015).

Meteorological conditions and parameters can have a significant impact on aerosol loading. As a result, weather conditions can throw off the AOD–$PM_{2.5}$ relationships.

From the correlation plots, we have examined that the aerosol loading increases with $PM_{2.5}$ increases. When particles are concentrated at the surface due to a low mix boundary layer height, AOD measurements may be low. Pollutants are better dispersed in the vertical column when the mix boundary layer is high, resulting in good agreement with AOD observations (Amarillo et al. 2021). The negative correlation between AOD and $PM_{2.5}$ over SI could be attributed to thermal inversion and the frequent occurrence of atmospherically elevated haze, such as fire plumes and dust, which may not be correlated to surface concentrations due to heterogeneity in the vertical profile or the fine mode fraction, as well as other factors that could cause AOD overestimation (errors in the MODIS cloud mask algorithm) (Pena and Araya 2019; Amarillo et al. 2021). The concentrations of $PM_{2.5}$ vary depending on the wind (air mass) reaching the selected study sites, so air quality is generally poor at AU, ARM, and GEC in the Indo-Gangetic Plains (Sarkar et al. 2018, 2019). Also, $PM_{2.5}$ concentrations are measured negatively associate with total precipitation for all locations except ARM.

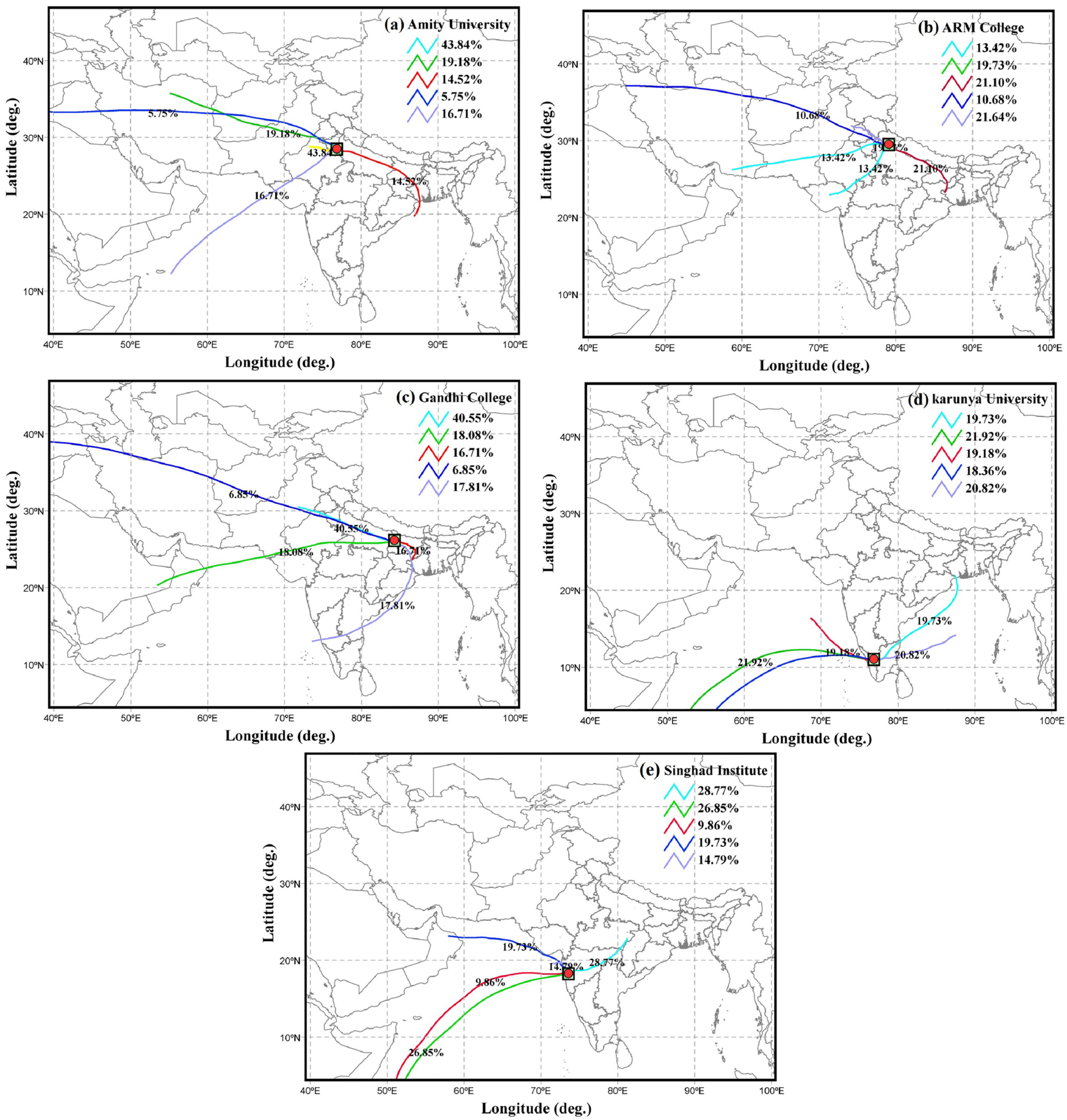

Fig. 4 Cluster analysis of 5 days airmass back trajectories for all five study locations, such as Amity University, ARM College, Gandhi College, Karunya University, and Singhad Institute

Figure 4 demonstrates the cluster analysis of 5 days airmass back trajectories arriving from different regions, ending at the altitude of 500 m (above ground level) AGL for all five locations Amity University, ARM College, Gandhi College, Karunya University, and Singhad Institute during only recent study year 2021. The Hybrid Single-Particle Lagrangian Integrated Trajectories (HYSPLIT) model was used to calculate the 5 days back trajectories of airmass and input meteorological data were used acquired from Global Data Assimilation System (GDAS, 1° × 1°) of National Oceanic and Atmospheric Administration (NOAA). Figure 4a shows the cluster analysis of 5 days airmass back trajectories for Amity University. Most of the contribution (~ 50–60%) of airmass is arriving from arid and semi-arid regions of western and central Asia, including Iraq, Iran, Afghanistan, and Pakistan for whole year of 2021. Also, 16.71% contribution of airmass is arriving from South-westerly regions Arabian Sea and 14.52% arriving from South-easterly regions Bay of Bengal passing through West Bengal, Jharkhand, Bihar, and Uttar Pradesh. Figure 4b shows the cluster analysis of 5 days airmass back trajectories for ARM College. This figure shows most of the contribution (~ 40–50%) of airmass is arriving from arid and semi-arid regions of western and central Asia. While 21.10% contribution of airmass is arriving from South-easterly regions. Figure 4c shows the cluster analysis of 5 days airmass back trajectories for Gandhi College. In this figure, most of the contribution (~ 70%) of airmass is arriving from arid and semi-arid regions of western and central Asia and also western part of India. While ~ 30% contribution of airmass is arriving from South-easterly regions and Passing through Arabian Sea to Bay of Bengal. Finally, Figs. 4d and 3e show the cluster analysis of 5 days airmass back trajectories for Karunya University and Singhad Institute, respectively. These figures show the almost same direction of airmass contribution as ~ 50–60% arriving from Arabian Sea and ~ 30–40% from Bay of Bengal. We have measured almost the same contribution of airmass from different regions for Amity University, ARM College, and Gandhi College while same for both Karunya University and Singhad Institute; the three dominant different regions of arriving airmass as arid and semi-arid regions of western and central Asia, south-westerly regions as Arabian Sea, and South-easterly regions as Bay of Bengal. Earlier studies (Datta et al. 2010; Xue et al. 2013) revealed that Asian dust, VOCs, and anthropogenic pollutants are present in the transported contaminated air mass from Eurasia and the Gulf countries.

5 Conclusions

This research's primary goal is to understand better the relationship between AOD, $PM_{2.5}$, temperature, relative humidity, and total precipitation. Solid particles always predictably play an authoritative role in the rainfall pattern of a particular area and season. The maximum rainfall has been observed for monsoon months (June–August) and post-monsoon months (October) for all locations during the study period. The maximum total precipitation has been measured for SI 11,674.7 (mm) and the minimum for KU 4563.41 (mm). The present study has been concentrated on the trends of AOD, $PM_{2.5}$, temperature, relative humidity, and total precipitation over the years 2015–2021 and assessed the impacts of AOD and $PM_{2.5}$ over rainfall and temperature. The study's outcomes mentioned the slightly incremental profile of AOD due to urbanization trends and transportation activities near the rural monitoring sites. This study explicitly revealed that correlations of AOD (550 nm) with $PM_{2.5}$, temperature, relative humidity, and total precipitation have a significant positive correlation for all locations. However, the correlations of $PM_{2.5}$ with temperature have a moderate positive correlation, whereas those with relative humidity and total precipitation have a negative correlation for all given locations except ARM college. We have measured almost same contribution of airmass from different regions for Amity University, ARM College, and Gandhi College while same for both Karunya University and Singhad Institute; the three dominant different regions of arriving airmass as arid and semi-arid regions of western and central Asia, south-westerly regions as Arabian Sea, and South-easterly regions as Bay of Bengal. This study thus highlights the necessity of taking into account the evolution of aerosols in future regional climate simulations.

Acknowledgements Authors thanks NASA, USA and Karunya Institute of Technology and Sciences, Coimbatore, India for required data research facilities.

Declarations

Conflict-of-interest The authors declare that they have no competing interests.

References

Ackerman AS, Toon OB, Stevens DE, Heymsfield AJ, Ramanathan V, Welton EJ (2000) Reduction of Tropical Cloudiness by Soot. Sci 288:1042–1047

Alfaro B, Limon ́R, Martínez T, Ramos G, Reyes A, Tijerina M (2008) Ciencias del ambiente. Patria, M ́exico, p. 363.

Amarillo A, Carreras H, Krisna T, Mignola M, Busso IT, Wendisch M (2021) Exploratory analysis of carbonaceous PM2.5 species in urban environments: Relationship with meteorological variables and satellite data. Atmos Environ 245:117987

Arora AS, Reddy AS (2013) Multivariate analysis for assessing the quality of stormwater from different Urban surfaces of the Patiala city, Punjab (India). Urban Water J 10(6):422–433

Arora AS, Reddy AS (2014) Development of multiple linear regression models for predicting the stormwater quality of urban subwatersheds. Bul Environ Contam Technol 92:36–43

Arora AS, Reddy AS (2015) Conceptualizing a decentralized stormwater treatment system for an urbanized city with improper stormwater drainage facilities. Int J Environ Sci Technol 12:2891–2900

Bisht L, Gupta V, Singh A, Gautam AS, Gautam S (2022) Heavy metal concentration and its distribution analysis in urban road dust: A case study from most populated city of Indian state of Uttarakhand. Spat. Spatio-Temp Epidemiol 40:100470

Chauhan A, Singh RP (2020) Decline in PM2.5 concentrations over major cities around the world associated with COVID-19. Environ Res 187:109634. https://doi.org/10.1016/j.envres.2020.109634

Chauhan A, Singh RP (2021) Effect of Lockdown on HCHO and Trace Gases over India during March 2020. Aerosol Air Qual Res 21:200445

Chelani A, Gautam S (2021) Lockdown during COVID-19 pandemic: A case study from Indian cities shows insignificant effects on urban air quality. Geosci Front. https://doi.org/10.1016/j.gsf.2021.101284

Chelani A, Gautam S (2022) The influence of meteorological variables and lockdowns on COVID-19 cases in urban agglomerations of Indian cities. Stoch Environ Res Risk Assess. https://doi.org/10.1007/s00477-021-02160-4

Chung CE, Ramanathan V, Kim D, Podgorny IA (2005) Global anthropogenic aerosol direct forcing derived from satellite and ground-based observations. J Geophys Res 110:D24207

Copernicus Climate Change Service (C3S) (2017) ERA5: Fifth generation of ECMWF atmospheric reanalyses of the global climate. Copernicus Climate Change Service Climate Data Store (CDS), 12–01–2022. https://cds.climate.copernicus.eu/cdsapp#!/home. Accessed Jan 2022

Datta A, Saud T, Goel A, Tiwari S, Sharma SK, Saxena M, Mandal TK (2010) Variation of ambient SO2 over Delhi. J Atmos Chem 65(2):127–143

Dey S, Tripathi SN, Singh RP, Holben BN (2004) Influence of dust storms on the aerosol optical properties over the Indo-Gangetic Basin. J Geophys Res 109:D20211

Gautam S, Gautam AS, Singh K, James EJ, Brema J (2021a) Investigations on the relationship among lightning, aerosol concentration, and meteorological parameters with specific reference to the wet and hot humid tropical zone of the southern parts of India. Environ Technol Innov. https://doi.org/10.1016/j.eti.2021.101414

Gautam AS, Tripathi SN, Joshi A, Mandariya AK, Singh K, Mishra G, Ramola RC (2021b) First surface measurement of variation of Cloud Condensation Nuclei (CCN) concentration over the Pristine Himalayan region of Garhwal, Uttarakhand, India. Atmos Environ 246:118123

Gautam S, Patra AK, Brema J, Raj PV, Raimond K, Abraham SS, Chudugudu KR (2021c) Prediction of various sizes of particles in deep opencast copper mine using recurrent neural network: a machine learning approach. J Inst Eng (india) Ser A. https://doi.org/10.1007/s40030-021-00589-y

Gollakota ARK, Gautam S, Santosh M, Sudan HA, Gandhi R, Jebadurai VS, Shu CM (2021) Bioaerosols: characterization, pathways, sampling strategies, and challenges to geo-environment and health. Gondwana Res 99:178–203. https://doi.org/10.1016/j.gr.2021.07.003

He J, Zha Y, Zhang J, Gao J, Wang Q (2014) Synergetic retrieval of terrestrial AOD from MODIS images of twin satellites Terra and Aqua. Adv Sp Res 53:1337–1346

Humbal C, Gautam S, Trivedi U (2018) A review on recent progress in observations, and health effects of Bioaerosols. Environ Int 118:189–193

Humbal C, Gautam S et al (2019) Evaluating the colonization and distribution of fungal and bacterial bioaerosol in Rajkot, western India using multi-proxy approach. Air Qual Atmos Health 12(6):693–704

Kalpana P, Prathibha S, Gopinathan P, Subramani T, Roy PD, Gautam S, Brema J (2020) Spatio-temporal estimation of rainfall patterns in north and northwestern states of India between 1901 and 2015: change point detections and trend assessments. Arab J Geosci 13:1116

KaufmanYJ KI, Remer LA, Rosenfeld D, Rudich Y (2005) The effect of smoke, dust, and pollution, aerosol on shallow cloud development over the Atlantic Ocean. Proc Nat Acad Sci USA 102:11207–11212

Kumar A (2015) Aerosols-cloud properties in dynamic atmosphere over Kedarnath Sub-Himalayan Region of India: a long term study from MODIS Satellite. Nat Environ Pollut Technol 14:493–500

Lau KM, Ramanathan K, Wu GX, Li Z, Tsay SC, Hsu C, Sikka R, Holben B, Lu D, Tartari G, Chin M, Koudelova P, Chen H, Ma Y, Huang J, Taniguchi K, Zhang R (2008) The joint aerosol monsoon experiment—a new challenge for monsoon climate research. Bull Am Meteorol Soc 89:369–383

Li J, Huang K, Wang Q, Lin Y, Xue F, Huang J, Fu SJ, Zhuang G (2010) Characteristics and source of black carbon aerosol over Taklimakan Desert. Sci China Chem 53:1202–1209

Meehl GA, Arblaster JM, Collins WD (2008) Effects of black carbon aerosols on the Indian Monsoon. J Clim 21:2869–2882

Menon S, Hansen J, Nazarenko L, Luo Y (2002) Climate effects of black carbon aerosols in China and India. Sci 297:2250–2253

Pena MA, Araya P (2019) Hacia el modelado de material particulado fino en Santiago, Chile, mediante im´ agenes MODIS. Rev. Geogr. Chileerra Aust 55 (1): 74–81. G:/Mi %20unidad/papers/trabajo%20CC%20completo%20traducido/revision/papers/28-Article%20Text-398–1–10–20191231.pdf.

Ramanathan V, Crutzen PJ, Kiehl JT, Rosenfeld D (2001a) Aerosols, climate and the hydrologic cycle. Sci 294:2119–2124

Ramanathan VC, Crutzen PJ, Kiehl JT, Rosenfeld D (2001b) Aerosols, climate, and the hydrological cycle. Sci 294:2119–2124

Ramanathan V, Chung C, Kim D, Bettge T, Buja L, Kiehl JT, Washington WM, Fu Q, Sikka DR, Wild M (2005) Atmospheric brown clouds: impacts on South Asian climate and hydrological cycle. Proc Nat Acad Sci USA 102:5326–5333

Ramasubramanian M (1998) Study of SO2 and no2 levels in some selected zones of Madurai City, Master Thesis, School of Energy Sciences, Madurai Kamaraj University, Madurai, India

Ranjan RR, Joshi HP, Iyer KN (2007) Spectral variation of total column aerosol optical depth over rajkot: a tropical semi-arid Indian Station. Aerosol Air Qual Res 7:33–45

Sarkar S, Singh RP, Chauhan A (2018) Crop residue burning in northern India: Increasing threat to Greater India. J Geophys Res 123:6920–6934

Sarkar S, Chauhan A, Kumar R, Singh RP (2019) Impact of deadly dust storms (May 2018) on air quality, meteorological, and atmospheric parameters over the northern parts of India. Geo Health 3:67–80

Tiwari S, Singh AK (2013) Variability of aerosol parameters derived from ground and satellite measurements over Varanasi located in the Indo-Gangetic Basin. Aerosol Air Qual Res 13:627–638

Xia XA, Chen HB, Wang PC, Zong XM, Gouloub P (2005) Aerosol Properties and their spatial and temporal variations over north China in Spring 2001. Tellus Ser B 57:28–39

Xie Y, Zhang Y, Xiong X, Qu JJ, Che H, Xie Y, Zhang Y, Xiong X, Qu JJ, Che H (2011) Validation of MODIS aerosol optical depth product over China using CARSNET measurements. Atm Environ 45:5970–5978

Xue LK, Wang T, Guo H, Blake DR, Tang J, Zhang XC, Wang WX (2013) Sources and photochemistry of volatile organic compounds in the remote atmosphere of western China: results from the Mt. Waliguan Observatory. Atmos Chem Phys 13(17):8551–8567